

NASA Technical Memorandum 102124
AIAA-89-2719

Structural and Thermal Response of 30 cm Diameter Ion Thruster Optics

G.S. MacRae, R.J. Zavesky, and S.T. Gooder
Lewis Research Center
Cleveland, Ohio

Prepared for the
25th Joint Propulsion Conference
cosponsored by the AIAA, ASME, SAE, and ASEE
Monterey, California, July 10-12, 1989



(NASA-TM-102124) STRUCTURAL AND THERMAL
RESPONSE OF 30 cm DIAMETER ION THRUSTER
OPTICS (NASA, Lewis Research Center) 29 p
CSCL 21C

N89-27703

Unclas

G3/20 0225957

STRUCTURAL AND THERMAL RESPONSE OF 30 CM DIAMETER ION THRUSTER OPTICS

G. S. MacRae, R. J. Zavesky and S. T. Gooder
National Aeronautics and Space Administration
Lewis Research Center
Cleveland, Ohio

ABSTRACT

This paper presents tabular and graphical data intended for use in calibrating and validating structural and thermal models of ion thruster optics. A 30 cm diameter, two electrode, mercury ion thruster was operated using two different electrode assembly designs. With no beam extraction, the transient and steady state temperature profiles and center electrode gaps were measured for three discharge powers. The data showed that the electrode mount design had little effect on the temperatures, but significantly impacted the motion of the electrode center. Equilibrium electrode gaps increased with one design and decreased with the other. Equilibrium displacements in excess of 0.5 mm and gap changes of 0.08 mm were measured at 450 W discharge power. Variations in equilibrium gaps were also found among assemblies of the same design. The presented data illustrate the necessity for high fidelity ion optics models and development of experimental techniques to allow their validation.

INTRODUCTION

Ion thrusters can deliver specific impulses from 2000 to 5000 seconds which makes them an attractive alternative to chemical rocket systems for orbit transfers, interplanetary missions, and other roles not requiring or not desiring high thrust levels.¹ Development efforts have increased and continue to increase the thrust delivered by ion thrusters. Space Electric Rocket Test I (SERT I) thrusters produced 25 mN thrust with a 10 cm ion extraction diameter or about 3 N/m².² SERT II thrusters produced 27 mN with a 14 cm ion extraction diameter, or 2 N/m².³ Today's 30 cm diameter, xenon thrusters produce 500 mN thrust or 7 N/m².⁴

These increases in thrust per unit area and thruster area are largely due to advances in ion optics design. The early electrodes (ion optics) used on SERT I and SERT II were flat and subject to severe, uncontrolled buckling when the radial temperature gradient became large. These factors limited the ability to scale the planar electrodes to large diameters and high thrust levels. By dishing the electrodes,⁵ the first buckling mode can be controlled, allowing reductions in electrode gap and thickness.⁶ Because the beam extraction is space charge limited,^{7,8} gap and grid thickness reductions translate into higher thrust per unit area as shown by Rawlin⁹ (Fig. 1). Greater control over the buckling and gap size also allows larger electrodes and higher thrusts to be achieved.

These advances were made with minimal computer aided structural analysis, and even less experimental measurement of deformations. Hughes Aircraft Company¹⁰ and Loral Electro-Optic Systems (EOS)¹¹ both developed finite element structural models of two and three electrode ion optics systems. Loral EOS also made displacement measurements of electrode gaps using an optical system.¹¹ Unfortunately, the uncertainty associated with those measurements was unquantified. With large circular and non-circular electrodes now under consideration, computer modeling is both an economical and essential step in advancing ion thruster design. The difficulty with most of these models is calibration and verification of the

predictions. The primary objective of this paper is to report experimental data to facilitate modeling efforts.

This paper presents data taken using a 30 cm diameter, divergent field, mercury ion thruster without extracting a beam. Transient and steady state thermal and displacement data were taken for two different electrode assembly designs.

APPARATUS

Three electrode assemblies of two different designs were used in the tests. The electrode assemblies consisted of two electrodes, insulators, and a mounting ring. The inner (screen) electrode was maintained at the cathode potential and the outer (accelerator) electrode was usually held a few hundred volts negative of the neutralizer potential. The insulators provided electrical isolation between the electrodes and the mounting ring fixed the cold electrode gap.

Four major design iterations were made in the development of a 3 kW mercury ion thruster for planetary propulsion applications.^{12,13,14} The 900-series and J-series, which were fabricated in the late 70's, were the last two. Both assemblies used identical electrodes and insulators with different mounting and stiffening rings. Because of an effort to reduce mass, the 900 series mounting ring was all titanium, and the screen electrode was mounted directly with screws. (Figs. 2 and 3). A thin molybdenum stiffening ring provided the interface between the accelerator electrode and the titanium portion of the mounting ring. The J-series design added a thick molybdenum stiffening ring to the screen electrode and increased the size of the stiffening ring on the accelerator electrode interface. The J-series molybdenum stiffening rings were attached to the electrodes with rivets and to the titanium ring with screws (Figs. 4 and 5). The titanium ring was redesigned for manufacturing ease and slotted to reduce the stiffness.

A three step process was used to manufacture the electrodes. First, a photoresist pattern was applied to the molybdenum sheets and the patterned sheets were then dished hydrostatically to a depth of 22 mm to control buckling. Then, circular ion extraction holes were chemically etched in the dished sheets.^{5,15} All electrode dimensions are shown in Table I. The screen electrode open area was high, 67 percent, to maximize ion extraction, while the accelerator open area was lower, 24 percent, to minimize neutral particle losses. The screen electrode hole pattern was sized down by 0.35 percent to intentionally misalign the screen and accelerator holes. This misalignment was intended to compensate for misalignments caused by the dishing procedure and to steer the beamlets to reduce beam divergence.¹⁶

PROCEDURE

A 30 cm diameter, divergent field, mercury ion thruster was operated in a 21 m long, 7.6 m diameter diffusion pumped vacuum chamber at NASA Lewis Research Center. Current regulated supplies were used to maintain the discharge, and there was no beam extraction. After preheating the mercury vaporizers on the cathode, neutralizer, and main flow systems, the discharge was initiated and the anode current, J_a , was fixed at a value determined by the beam current, J_b , being modeled. The mercury flow through the cathode was then adjusted to bring the discharge voltage, V_d , to 32 V. Only about 5 percent of the mercury vapor flowed through the cathode as the main portion was injected directly into the discharge chamber. The main mercury flow rate was fixed at approximately the values that would be required to achieve the beam current that corresponds to the anode current used. With ion beam extraction, the discharge power, P_d , is the product of the discharge voltage and the difference between the anode current and beam current. Because no beam was extracted during the testing, the formula for discharge power was simply:

$$P_d = V_d J_d. \quad (1)$$

For a more complete description of ion thruster techniques, set points, and logic, see Ref. 14.

Temperature Measurements

Two electrode assemblies, the 900-series (SN813) and the J-series (SN842), were configured with 10 chromel-alumel thermocouples, of which three were attached to each of the electrodes and four to the mounting rings (Figs. 6 and 7 for the 900 and J-series respectively). The thermocouples were located at the same radial positions to simplify comparisons of the 900 and J-series assemblies. Transient and steady state temperatures were measured at three power levels for both assemblies. For all tests, the same 30 cm diameter discharge chamber was used.

Data could not be taken continuously, so the exact times required to reach equilibrium temperatures were not always available. The data presented, therefore, employ two artificial time constants. The time constant definitions were based on the assumption that an exponential equation of the form:

$$T = \Delta T (1 - e^{-t/T_c}) + T_i \quad (2)$$

governed the temperature change, where T was the temperature at time t , ΔT was the difference between the equilibrium temperature and the temperature at cathode ignition, T_i , and T_c was the time constant. The 63.2% time constant was defined exactly as in Eq. 2, and was the time required for the temperature to reach 63.2 percent of the difference between the equilibrium and cathode ignition temperatures. The 95% time constant was the time required to reach 95 percent of the temperature difference. The 95% time constant would be three times the 63.2% time constant if Eq. 2 described the temperature function exactly. The distribution of the data made the 95% time constant more accurate than the 65% time constant.

All transient data were referenced to cathode ignition time, for two reasons. It was explicitly known for all of the test runs, while the preheat times, wherein the mercury vaporizers heated, varied for the tests. In addition, the presence of the discharge was the dominant factor in determining the temperatures of the ion optics.

Displacement Measurements

Thermally induced displacements were measured for three electrode assemblies. Two of these, the 900-series (SN813) and J-series (SN842) assemblies, were instrumented with thermocouples for simultaneous measurement of the temperature profiles. The last assembly, J-series (SN903), was tested without thermocouples. It was chosen for tests because it demonstrated the most efficient beam extraction capability of the J-series assemblies available.

Displacements were measured using a stepper motor driven probe that contacted either the accelerator electrode or a post extending from the screen electrode (Figs. 8 and 9). The measuring system was rigidly attached to the discharge chamber, as shown in Figure 10. The motion of the reference location of the measuring system was uncompensated and unknown. Thus, to remove any error introduced by motion of the reference position, the gap, or difference between the measurements of the screen and accelerator electrode locations, was used to compare displacements for different designs and discharge powers.

The probe was a 7.9 thread per cm jack screw actuator driven by a variable reluctance, 15°/step stepper motor with a 97:1 gear box. Probe contact was confirmed when an electrical circuit

between the electrode and the probe was closed. Each actuator had a sensitivity of 47 pulses per 0.0025 cm of motion. A hysteresis or dead band occurred when the motion was reversed. The screen and accelerator actuators had dead bands of 110 and 115 pulses, respectively. The dead bands were calibrated using a dial indicator accurate to 0.0013 cm. Displacement measurements were made at the electrode centers on the thruster axis. The actuator controller drove both stepper motors independently and simultaneously. The total uncertainty of the centerline gap measurement was about 0.0025 cm.

No ion beam was extracted because it would have had detrimental effects on the displacement measuring equipment which was installed in the center of the beam path.

RESULTS

The data presented are intended for use in calibrating and verifying models used to predict electrode response. For that reason, data are presented in figure and tabular form. Some of the data are omitted from certain figures to improve clarity. All of the data were taken without ion beam extraction to provide direct comparison for the temperatures and electrode gap measurements for use in modeling efforts.

Temperature Measurements

Table II shows transient temperature profiles measured at discharge powers of 210, 350, and 493 W for the 900-series assembly. Figures 11 through 13 show the temperatures measured at selected thermocouples. All times were normalized to cathode ignition at 0 minutes in order to provide a consistent, accurate reference for comparisons. The heating before the cathode was ignited was due to the vaporizer heaters. After ignition, the temperatures rose exponentially towards their equilibrium values. 65% and 95% time constants were extracted for each of the thermocouples on the 900 series electrode (Table III). Figure 14 shows the 95% time constants for two discharge powers. The time constants increased monotonically from the center to the edge of the screen electrode with a variation of more than a factor of 2.5. Across the mounts, the fractional variation in time constants was smaller but all were higher than the electrode constants. Again time constants increased monotonically with radial location. The time constants from the accelerator electrode were close to, but slightly higher than those of the screen electrode. As will be discussed later, these results strongly affected the transient electrode spacing.

The J-series design showed similar transient thermal characteristics. Transient temperatures are shown in Table IV and Figure 15 for a 210 W discharge. The 95% time constants are given in Table V and compared with values from the 900-series electrode in Figure 16. The J-series assembly demonstrated a smaller spread of time constants than the 900-series. This was likely due to the higher initial temperatures for the J-series test. The discharge was initiated about 20 minutes earlier than shown in figure 16 but, was held at a low power until the indicated cathode ignition time. Again, if the accelerator and screen electrode locations are treated separately, the time constants increased monotonically with the radius.

The temperature measurements described above were taken without displacement measurements. This allowed documentation of the transient temperatures at all of the thermocouple locations. The following temperature measurements were taken concurrently with displacement measurements, using the same electrode assemblies. The labor intensive method of controlling the displacement measurement interfered with temperature measurement records so transient temperatures were measured only on the electrode centerlines. Comparisons of the transient centerline temperature measurements in Tables VI and VII show good agreement with the equivalent temperatures shown in Tables II and IV. When equilibrium was reached, temperatures were recorded for all of the thermocouples. Of the data presented,

the data from Table VIII provide the highest fidelity and should be used for steady state values to compare model predictions with displacement measurements.

Transient temperature data on the 900-series (SN813) and J-series (SN842) assembly centerlines are shown in Tables VI and VII and Figures 17 and 18. Again, the transient response is almost identical for the two designs. For all discharge powers and designs tested, the electrode assemblies heated to their equilibrium temperatures within 100 minutes of initiating a discharge.

Steady state temperatures for the two assemblies are shown in Table VIII and figure 19 for discharge powers from 210 to 450 W. The figures show that, for a given power level, the only significant difference in temperatures occurred near the transition from molybdenum to titanium on the mounting ring. The molybdenum support ring on the J-series design maintained a higher temperature than the equivalent position on the titanium mounting ring of the 900-series design.

Displacement Measurements

Transient electrode motion and spacing changes are shown in Tables VI and VII and Figures 20 and 21. The electrode gap was reduced initially for both the 900 and J-series assemblies, then the gap opened to the equilibrium value. Transient displacements of the screen electrode of more than 0.8 mm and transient gap reductions of more than 0.25 mm were measured. Both the rate and magnitude of the gap changes were complex. The initial gap reduction was due to rapid heating of the screen electrode. With the 900-series assembly, the magnitude of the initial gap change varied inversely with discharge power. The magnitude of the initial gap change of the J-series assembly did not vary monotonically discharge power. The time required for the minimum gap to be reached, for both assemblies, seemed to increase with discharge power increases. The complex response characteristics were probably due to the variations in thermal equilibration times for points at different radii on the assemblies.

Equilibrium gap changes are reported in Table IX for a 900 and two J-series assemblies. The equilibrium gap is plotted in Figure 22 for the same conditions. The equilibrium gaps for a given assembly were reproducible to within the accuracy of the measuring system for all power levels tested. The 900 and J-series assemblies had distinctly different responses. The 900-series gap increased at all power levels between 200 and 450 W and the J-series gaps all decreased at those power levels. This appears to be due to design differences, specifically, the addition of a molybdenum support ring and weakening of the titanium ring on the J-series design. With its higher expansion coefficient, the 900-series titanium mounting ring put the screen electrode under tension at the edge, which reduced the absolute motion of the electrode center.

It is difficult to account for the differences in the responses of the two J-series assemblies. While the first J-series assembly demonstrated a monotonic response to discharge power, the second did not. The gap change of the second assembly was greater than that of the first and nearly constant. This suggests that the initial states of the electrodes were different.

CONCLUSIONS

The electrode designs under consideration for future ion thrusters make computer modeling both an economical and essential step in advancing the state of the art. The largest road block to these efforts is the scarcity of experimental data to calibrate and validate the models. This paper presented transient and steady state thermal and displacement data from tests of a 30 cm diameter, mercury ion thruster operated without beam extraction. The fidelity of the steady state data was ensured by recording the displacement and thermal data simultaneously. The

transient centerline temperatures measured concurrently with displacement measurements closely matches the transient thermal data recorded independently of the displacement measurements.

Experimental data to calibrate and validate finite element models of ion thruster optics systems are presented. Except for one thermocouple location on the mounting rings, the temperature measurements show little difference between the equilibrium or transient temperatures of the two electrode assembly designs tested. Across the radius of the assembly, the time constants vary by as much as a factor of four, increasing monotonically with the radius. The highest 95% time constants were less than 100 minutes for all assemblies and power levels tested and increasing the discharge power reduced the time constants.

Transient electrode motions were found to be very complex. The general pattern was for the gap to decrease a large amount initially and then approach the equilibrium gap which could be larger or smaller than the initial gap depending on the electrode design. Transient displacements as high as 0.8 mm for the screen electrode and transient gap reductions as high as 0.25 mm were measured. Steady state gap changes as large as 0.08 mm and motions of 0.5 mm were measured.

The equilibrium electrode motions were very different for the two designs. The electrode gap increased from the cold gap at operating temperatures in one design while the gap decreased with the other design. The equilibrium gap was also found to vary significantly among assemblies of the same design. The difference in responses of the two designs should be predictable with modeling. The variation within a design may be due to the initial states of the hardware which most likely must be addressed by improved controls on manufacturing, assembly, and handling processes. The data of this report indicate the necessity of high fidelity ion optics models and further development of experimental techniques to allow their validation.

REFERENCES

- 1 Stone, J. R., Byers, D. C. and King D. Q., "The NASA Electric Propulsion Program," Proceedings: 20th International Electric Propulsion Conference, October 1988, pp. 17-25.
- 2 Cybulski, R. J., "Results from SERT I Ion Rocket Flight Test," NASA TN D-2718, March 1965.
- 3 Kerslake, W. R., Byers, D. C. and Staggs, J. R., "SERT II Experimental Thrustor System," AIAA Paper 67-700, September 1967.
- 4 Patterson, M. J. and Rawlin, V. K., "Performance of 10 kW Class Xenon Ion Thrusters," AIAA Paper 88-2914, July 1988.
- 5 Rawlin, V. K.; Banks, B. A. and Byers, D. C., "Design, Fabrication, and Operation of Dished Accelerator Grids on a 30 cm Ion Thruster," Journal of Spacecraft and Rockets, Vol. 10, No. 1, January 1973.
- 6 Rawlin, V. K., "Studies of Dished Accelerator Grids for 30 cm Ion Thrusters," AIAA Paper 73-1086, October 1973.

- 7 Kaufman, H. R., "Technology of Electron-Bombardment Ion Thrusters," Advances in Electronics and Electron Physics, Vol. 36, Academic Press, New York, 1974.
- 8 Rawlin, V. K., "Sensitivity of 30 cm Mercury Bombardment Ion Thruster Characteristics to Accelerator Grid Design," AIAA Paper 78-688, April 1978.
- 9 Rawlin, V. K., "Studies of Dished Accelerator Grids for 30 cm Ion Thrusters," AIAA Paper 73-1086, October, 1973.
- 10 Poeschel, R. L. and Kami, S., "Analysis and Design of Ion Thrusters for Large Space Systems," NASA CR-165140, September 1980.
- 11 James, E. L.. et al, "Advanced Inert Gas Ion Thrusters," NASA CR-168192, July 1984.
- 12 Poeschel, R. L., "Retrofit and Acceptance Test of 30 cm Ion Thrusters," NASA NAS3-21357, June 1981.
- 13 "30 cm Ion Thruster Subsystem Design Manual," NASA TM-79191, June 1979.
- 14 Schnelker, D. E., Collet, C. R., Kami, S. and Poeschel, R. L., "Characteristics of the NASA/Hughes J-Series 30 cm Engineering Model Thruster," AIAA Paper 79-2077, October 1979.
- 15 Collet, C. R., "Fabrication and Verification Testing of ETM 30 cm Diameter Ion Thrusters," NASA CR-135193, April 1977.
- 16 Danilowicz, R. L., Rawlin, V. K., Banks, B. A. and Wintucky, E. G., "Measurement of Beam Divergence of 30 cm Diameter Dished Grids," AIAA Paper 73-1051, October 1973.

TABLE I. - ELECTRODE DIMENSIONS.

ELECTRODE ASSEMBLY		HOLE DIAMETER, MM		ELECTRODE THICKNESS, MM		OPEN AREA FRACTION		COMPEN-	RATIO OF DISH DEPTH TO DIAMETER
SERIES	SERIAL NUMBER	SCREEN	ACCELERATOR	SCREEN	ACCELERATOR	SCREEN	ACCELERATOR	SATION, STRAIN %	
900	813	1.91	1.14	0.38	0.38	0.67	0.24	0.35	0.075
J	842	1.91	1.14	0.38	0.38	0.67	0.24	0.35	0.075
J	903	1.91	1.14	0.38	0.38	0.67	0.24	0.35	0.075

* COMPENSATION IS THE REDUCTION OF THE CENTER TO CENTER HOLE SPACING OF THE SCREEN ELECTRODE EXPRESSED AS THE PERCENTAGE OF THE REDUCTION DISTANCE DIVIDED BY THE RADIAL LOCATION OF THE HOLE.

TABLE II. - TRANSIENT TEMPERATURE OF THE 900-SERIES SN813 ASSEMBLY.

A. - 210 W DISCHARGE POWER.

TIME, MIN	TEMPERATURES, °C									
	THERMOCOUPLE LOCATIONS REFERENCED TO FIG. 6									
	1	2	3	4	5	6	7	8	9	10
	RADIAL POSITION, CM									
	0.0	5.0	14.4	15.8	16.9	18.3	15.8	14.4	5.0	0.0
-26	22	22	22	22	22	22	22	22	22	22
-16	31	31	26	24	23	22	24	25	28	29
-6	55	52	39	31	27	24	31	36	46	49
-1	67	63	46	36	31	26	36	42	55	59
2	190	166	86	44	36	27	46	62	108	121
6	230	209	121	69	52	33	68	91	152	169
14	252	233	157	112	85	53	98	123	182	198
24	271	246	177	141	112	79	117	141	198	216
34	276	256	191	157	131	101	129	153	207	223
44	279	261	201	169	145	117	139	161	213	227
89	284	268	216	191	168	145	154	174	223	235
194	284	270	219	195	173	151	158	178	225	238
284	284	269	219	196	173	152	158	178	226	238

B. - 350 W DISCHARGE POWER.

TIME, MIN	TEMPERATURES, °C									
	THERMOCOUPLE LOCATIONS REFERENCED TO FIG. 6									
	1	2	3	4	5	6	7	8	9	10
	RADIAL POSITION, CM									
	0.0	5.0	14.4	15.8	16.9	18.3	15.8	14.4	5.0	0.0
-27	26	26	26	26	26	26	26	26	26	26
-17	34	34	30	27	26	26	27	29	32	33
-7	57	55	42	34	31	27	34	39	49	52
-2	71	67	50	39	34	29	39	45	59	63
1	227	203	98	46	38	31	47	66	124	134
3	283	256	138	66	51	33	67	98	186	207
6	291	267	162	97	71	41	91	124	207	229
10	328	310	200	133	97	55	114	153	244	263
16	345	322	231	179	135	83	141	178	265	284
23	349	333	249	204	163	113	157	194	276	291
33	354	338	263	224	187	144	173	207	283	297
48	358	343	274	241	207	170	186	217	290	302
98	362	347	284	255	224	192	197	227	297	308
133	363	348	285	256	225	193	198	228	297	309
233	361	348	286	257	231	194	199	229	298	309

C. - 493 W DISCHARGE POWER.

TIME, MIN	TEMPERATURES, °C									
	THERMOCOUPLE LOCATIONS REFERENCED TO FIG. 6									
	1	2	3	4	5	6	7	8	9	10
	RADIAL POSITION, CM									
	0.0	5.0	14.4	15.8	16.9	18.3	15.8	14.4	5.0	0.0
-32	23	23	23	23	23	23	23	23	23	23
-22	32	32	27	25	24	23	25	26	30	31
-17	43	42	33	28	26	23	28	31	38	40
-12	55	54	41	32	28	25	33	37	48	51
-7	68	64	47	37	32	27	37	43	56	61
-2	78	74	54	42	36	29	42	49	64	69
1	188	173	86	47	39	32	47	62	104	109
3	321	286	151	67	51	34	68	104	208	232
6	349	323	197	116	81	42	104	148	256	279
11	371	349	243	178	127	68	138	184	288	307
18	383	361	269	218	169	108	163	207	304	322
28	391	370	289	247	204	152	185	226	315	332
38	395	375	299	262	222	176	197	235	321	337
48	397	377	304	270	233	191	204	241	324	339
58	398	379	308	275	239	199	208	244	326	341
68	399	381	311	278	243	204	211	247	328	343
116	402	383	314	283	248	212	215	251	331	345
190	402	384	314	284	249	213	216	251	331	346
248	402	384	314	284	249	214	216	251	331	346

TABLE III. - 62.3% AND 95% TIME CONSTANTS FOR A 900-SERIES ELECTRODE ASSEMBLY.

THERMOCOUPLE LOCATIONS REFERENCED TO FIG. 6	RADIAL POSITION, CM	TIME TO REACH 63.2% OF FINAL TEMPERATURE, MIN			TIME TO REACH 95% OF FINAL TEMPERATURE, MIN		
		DISCHARGE POWER, W			DISCHARGE POWER, W		
		210	350	493	210	350	493
1	0.0	3	2	2	29	18	22
2	5.0	4	3	2	42	25	26
3	14.4	14	10	8	73	48	43
4	15.8	23	16	14	82	65	52
5	16.9	29	22	18	86	89	58
6	18.3	36	30	26	97	85	68
7	15.8	22	16	15	83	70	55
8	14.4	17	11	10	78	60	48
9	5.0	9	6	4	65	38	31
10	0.0	5	5	3	57	33	28

TABLE IV. - J-SERIES TRANSIENT TEMPERATURE PROFILES AT 210 W DISCHARGE POWER.

TIME, MIN	TEMPERATURES, °C									
	THERMOCOUPLE LOCATIONS REFERENCED TO FIG. 6									
	1	2	3	4	5	6	7	8	9	10
	RADIAL POSITION, CM									
	0.0	5.0	14.4	15.8	16.9	18.3	15.8	14.4	5.0	0.0
-57	23	23	23	23	23	22	23	23	22	23
-47	34	32	26	26	23	23	25	26	29	32
-37	59	54	38	37	26	25	33	36	46	51
-27	83	78	57	55	32	31	44	48	65	72
-17	101	94	73	72	39	38	56	60	79	87
-11	109	103	83	82	46	44	62	67	87	95
1	119	114	97	96	57	54	72	78	97	105
5	206	194	118	112	61	57	86	98	152	172
9	229	217	146	139	71	64	105	119	175	193
22	254	246	197	192	109	96	140	153	202	216
50	268	259	223	221	150	138	169	178	217	227
77	271	262	229	226	161	149	176	185	221	229
95	269	263	232	229	166	154	179	188	222	230
359	269	263	232	229	166	155	180	188	223	231
1279	269	262	232	229	166	155	180	188	222	230

TABLE V. - J-SERIES TIMES TO TEMPERATURES FOR A 210 W DISCHARGE POWER.

THERMOCOUPLE LOCATIONS REFERENCED TO FIG. 6	RADIAL POSITION, CM	TIME CONSTANT, MIN	
		63.2%	95%
		1	0.0
2	5.0	8	44
3	14.4	18	54
4	15.8	19	62
5	16.9	33	79
6	18.3	37	79
7	15.8	22	73
8	14.4	20	69
9	5.0	10	49
10	0.0	7	46

TABLE VI. - 900-SERIES SN813 ELECTRODE TRANSIENT DEFORMATIONS AND TEMPERATURES.

A. - 210 W DISCHARGE POWER.

TIME, MIN.	TEMPERATURES, °C		ELECTRODE MOTION, MM		ELECTRODE GAP, MM	EVENT
	SCREEN CENTER	ACCEL CENTER	SCREEN	ACCEL		
-30.8	19	19	0.00	0.00	0.51	PREHEAT
-28.7			0.03	0.03	0.51	
-21.3			0.05	0.01	0.51	
-16.5			0.08	0.08	0.51	
-11.8	48	42	0.10	0.10	0.51	
-6.7			0.13	0.13	0.51	CATHODE IGNITION
0.0	74	63	0.13	0.15	0.53	
0.8			0.28	0.20	0.43	
1.0			0.33	0.23	0.41	
1.3			0.38	0.25	0.38	
1.5			0.41	0.28	0.38	
2.0			0.48	0.31	0.33	
2.2			0.48	0.33	0.36	
2.5			0.51	0.33	0.33	
3.2			0.53	0.36	0.33	
3.8			0.53	0.38	0.36	
4.1			0.56	0.38	0.33	
4.3	225	161	0.56	0.41	0.36	
5.3			0.56	0.43	0.38	
8.3			0.56	0.46	0.41	
11.1			0.51	0.48	0.48	
13.2			0.48	0.48	0.51	
15.7			0.46	0.46	0.51	
20.4			0.43	0.46	0.53	
27.7			0.43	0.43	0.51	
29.0	223	224	0.41	0.43	0.53	
32.6	279	226	0.38	0.41	0.53	
121			0.36	0.38	0.53	210 W DISCHARGE EQUILIBRIUM
166			0.33	0.36	0.53	
250	286	238	0.33	0.36	0.53	
1196	285	238	0.33	0.36	0.53	

TABLE VI. - CONCLUDED.

B. - 350 W DISCHARGE POWER

TIME, MIN.	TEMPERATURES, °C		ELECTRODE MOTION, MM		ELECTRODE GAP, MM	EVENT
	SCREEN CENTER	ACCEL CENTER	SCREEN	ACCEL		
-25.7	22	22	0.00	0.00	0.51	PREHEAT
-21.6			0.03	0.03	0.51	
-15.4			0.05	0.05	0.51	
-10.4			0.08	0.08	0.51	
-5.2			0.10	0.10	0.51	
0.0	70	61	0.13	0.13	0.51	CATHODE IGNITION
2.5			0.25	0.18	0.43	
3.0			0.38	0.25	0.38	
3.5			0.51	0.28	0.28	
4.0			0.66	0.41	0.25	
4.8	292	216	0.74	0.53	0.30	
5.5			0.74	0.61	0.38	
6.1			0.76	0.64	0.38	
6.7			0.76	0.66	0.41	
10.3			0.64	0.69	0.56	
11.1	337	278	0.61	0.69	0.61	
12.4			0.58	0.69	0.61	
14.3			0.56	0.69	0.61	
19.3			0.53	0.66	0.64	
25.2			0.51	0.66	0.66	
35.8	354	303	0.51	0.64	0.64	350 W DISCHARGE EQUILIBRIUM
37.6			0.48	0.64	0.66	
1235			0.38	0.53	0.66	

C. - 450 W DISCHARGE POWER.

TIME, MIN.	TEMPERATURES, °C		ELECTRODE MOTION, MM		ELECTRODE GAP, MM	EVENT
	SCREEN CENTER	ACCEL CENTER	SCREEN	ACCEL		
-29.9	26	26	0.00	0.00	0.51	PREHEAT
-25.5			0.03	0.03	0.51	
-17.6			0.05	0.05	0.51	
-9.9			0.08	0.08	0.51	
0.0			62	56	0.10	
18.3	0.38	0.36			0.48	
20.1	0.76	0.61			0.41	
21.9	0.81	0.69			0.38	
23.3	353	282			0.81	0.71
24.4			0.79	0.71	0.43	
25.0			0.71	0.74	0.53	
26.1			0.69	0.74	0.56	
26.6			0.64	0.74	0.56	
27.1	391	334	0.61	0.74	0.64	
30.4			0.56	0.69	0.64	
52.8			0.53	0.69	0.66	
59.4			0.51	0.69	0.69	
60.3			0.51	0.69	0.69	
1045	396	343	0.41	0.58	0.69	450 W DISCHARGE EQUILIBRIUM

TABLE VII. - J-SERIES SN842 ASSEMBLY TRANSIENT DEFORMATIONS AND TEMPERATURES.

A. - 210 W DISCHARGE POWER

TIME, MIN.	TEMPERATURES, °C		ELECTRODE MOTION, MM		ELECTRODE GAP, MM	EVENT
	SCREEN CENTER	ACCEL CENTER	SCREEN	ACCEL		
-25.6	23	23	0.00	0.00	0.51	PREHEAT
-23.2			0.03	0.03	0.51	
-17.6			0.05	0.03	0.48	
-13.7			0.08	0.05	0.48	
-9.5			0.10	0.05	0.46	
-6.5			0.10	0.08	0.48	
-5.6			0.13	0.08	0.46	
-1.1	72	47	0.15	0.08	0.43	CATHODE IGNITION
0.0			0.10	0.10	0.51	
3.7			0.23	0.13	0.41	
4.0			0.28	0.13	0.36	
4.2			0.30	0.15	0.36	
4.4			0.38	0.18	0.30	
4.7			0.43	0.20	0.28	
5.0	180	87	0.46	0.20	0.25	
5.4			0.48	0.23	0.25	
5.8			0.51	0.25	0.25	
6.2			0.53	0.28	0.25	
6.8			0.53	0.30	0.28	
7.0			0.56	0.33	0.28	
8.1			0.56	0.36	0.30	
9.5	248	152	0.56	0.38	0.33	
11.3			0.51	0.41	0.41	
11.9			0.51	0.41	0.41	
12.4			0.48	0.41	0.43	
13.0			0.46	0.41	0.46	
15.5			0.46	0.43	0.48	
17.1			0.43	0.43	0.51	
20.8	267	178	0.43	0.41	0.48	
21.4			0.43	0.41	0.48	
25.4			0.41	0.41	0.51	
33.2	281	200	0.38	0.41	0.53	
40.7			0.36	0.38	0.53	
116	287	219	0.33	0.30	0.48	210 W DISCHARGE EQUILIBRIUM
202	288	221	0.30	0.28	0.48	
334	288	221	0.30	0.28	0.48	
1264	283	216	0.30	0.28	0.48	

TABLE VII. - CONTINUED.

B. - 350 W DISCHARGE POWER

TIME, MIN.	TEMPERATURES, °C		ELECTRODE MOTION, MM		ELECTRODE GAP, MM	EVENT
	SCREEN CENTER	ACCEL CENTER	SCREEN	ACCEL		
-26.3	26	26	0.00	0.00	0.51	PREHEAT
-22.6			0.03	0.03	0.51	
-15.5			0.05	0.05	0.51	
-12.2			0.08	0.05	0.48	
-7.5			0.10	0.08	0.48	
0.0	75	49	0.28	0.10	0.33	CATHODE IGNITION
2.7			0.23	0.13	0.36	
4.1	231	104	0.58	0.28	0.20	
4.2			0.61	0.30	0.20	
4.4			0.64	0.33	0.20	
4.7			0.66	0.36	0.20	
5.0			0.66	0.38	0.23	
5.4			0.69	0.41	0.23	
6.0	279	171	0.69	0.43	0.25	
6.3			0.69	0.46	0.28	
6.9			0.69	0.48	0.41	
7.7			0.69	0.51	0.33	
8.7			0.69	0.53	0.36	
10.8			0.69	0.56	0.38	
11.5	296	201	0.61	0.56	0.46	
13.4			0.58	0.56	0.48	
18.5			0.56	0.58	0.48	
21.3	327	240	0.53	0.56	0.48	
23.7			0.53	0.48	0.51	
27.4			0.51	0.53	0.53	
35.3			0.51	0.51	0.51	
45.0			0.51	0.48	0.48	
50.7	343	269	0.51	0.48	0.48	
1219			353	292	0.46	0.41

TABLE VII. - CONCLUDED.

C. - 450 W DISCHARGE POWER

TIME, MIN.	TEMPERATURES, °C		ELECTRODE MOTION, MM		ELECTRODE GAP, MM	EVENT
	SCREEN CENTER	ACCEL CENTER	SCREEN	ACCEL		
-29.6	23	23	0.00	0.00	0.51	PREHEAT
-25.6			0.03	0.03	0.51	
-16.9			0.05	0.05	0.51	
-9.4			0.10	0.08	0.48	
-1.2			0.13	0.10	0.48	
0.0	86	54	0.15	0.10	0.46	CATHODE IGNITION
6.0			0.41	0.36	0.46	
6.7			0.58	0.36	0.28	
7.5			0.74	0.38	0.15	
8.3			0.79	0.48	0.20	
8.6			0.79	0.51	0.23	
8.8			0.81	0.53	0.23	
9.4	324	224	0.81	0.56	0.25	
9.8			0.81	0.58	0.28	
10.5			0.81	0.61	0.30	
11.8			0.81	0.64	0.33	
13.8			0.81	0.66	0.36	
15.7			0.71	0.69	0.48	
17.0			0.69	0.69	0.51	
17.6			0.66	0.69	0.53	
20.8			0.64	0.66	0.53	
21.4	381	303	0.64	0.66	0.53	
27.8	391	313	0.61	0.64	0.53	
31.9			0.61	0.61	0.51	
32.9			0.58	0.61	0.53	
37.4	392	319	0.58	0.58	0.51	
52.4			0.58	0.53	0.46	
92.4	394	325	0.56	0.48	0.43	
136			0.56	0.46	0.41	
1302	397	327	0.53	0.46	0.43	450 W DISCHARGE EQUILIBRIUM

TABLE VIII. - TEMPERATURE PROFILE FOR DIFFERENT DISCHARGE POWERS, WITHOUT BEAM EXTRACTION.

THERMO-COUPLE LOCATION	THERMO-COUPLE NUMBER	RADIAL POSITION, CM	TEMPERATURE, °C					
			J-SERIES ELECTRODE ASSEMBLY			900-SERIES ELECTRODE ASSEMBLY		
			DISCHARGE POWER, W			DISCHARGE POWER, W		
			210	350	450	210	350	450
SCREEN	1	0.0	278	353	397	285	354	396
	2	5.0	266	346	381	268	333	376
	3	14.4	194	294	324	219	277	314
MOUNTING RING	4	15.8	191	291	319	193	246	279
	5	16.9	99	215	239	174	221	250
	6	18.3	83	196	216	154	158	216
	7	15.8	124	222	246	166	203	227
ACCELERATOR	8	14.4	137	234	259	178	221	249
	9	5.0	189	276	310	225	287	327
	10	0.0	209	292	327	238	303	343

• THERMOCOUPLE NUMBERS REFER TO FIGURES 7 AND 8 FOR THE 900 AND J-SERIES ASSEMBLIES RESPECTIVELY.
 • J-SERIES SN842 ELECTRODE ASSEMBLY WAS USED.
 • 900-SERIES SN813 ELECTRODE ASSEMBLY WAS USED.
 • DATA ARE FROM THE SECOND TEST SERIES.

TABLE IX. - EQUILIBRIUM ELECTRODE GAP CHANGE.

ELECTRODE ASSEMBLY		ABSOLUTE GAP CHANGE, MM		
SERIES	SERIAL NUMBER	DISCHARGE POWER, W		
		210	350	450
900	813	0.025 5%	0.15 30%	0.18 35%
J	842	-0.025 -5%	-0.051 -10%	-0.076 -15%
J	903	-0.18 -35%	-0.18 -35%	-0.15 -30%

• NEGATIVE DISPLACEMENTS INDICATE A DECREASING ELECTRODE GAP.
 • PERCENTAGES REFLECT THE CHANGE RELATIVE TO THE INITIAL GAP OF 0.51 MM.
 • NO ION BEAM EXTRACTION.

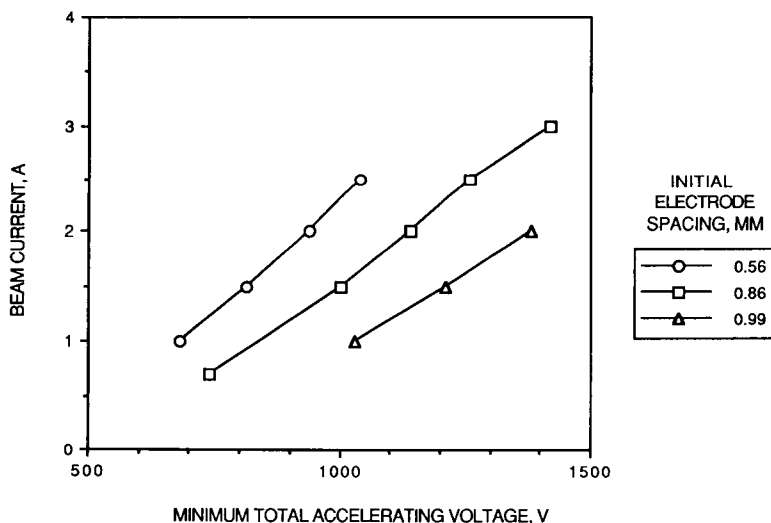


FIGURE 1. - BEAM EXTRACTION SENSITIVITY TO ELECTRODE SPACING, REF. 9.

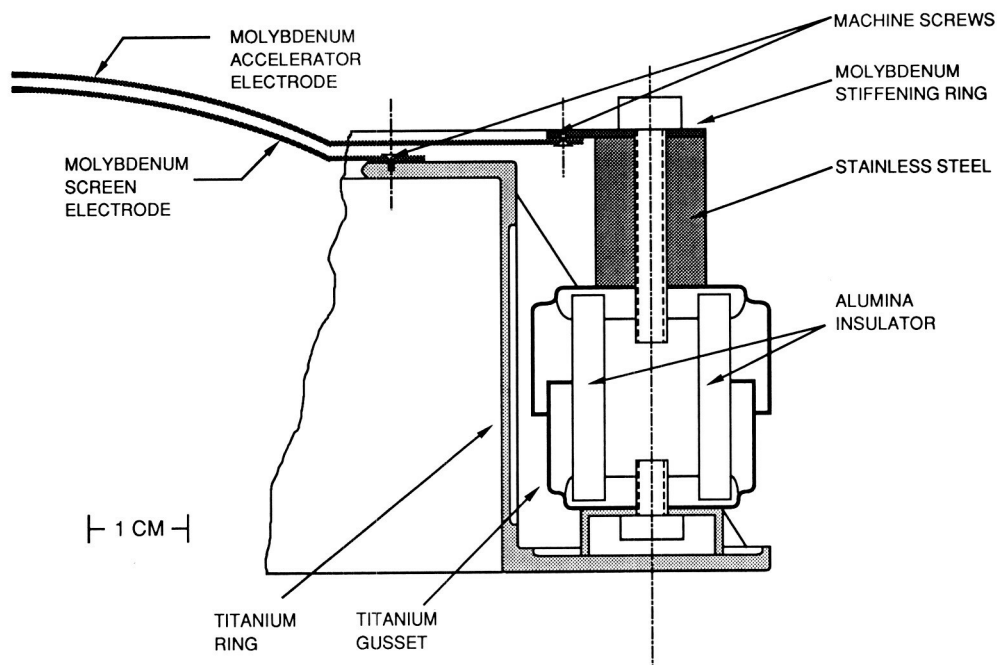


FIGURE 2. - 900-SERIES ELECTRODE ASSEMBLY.

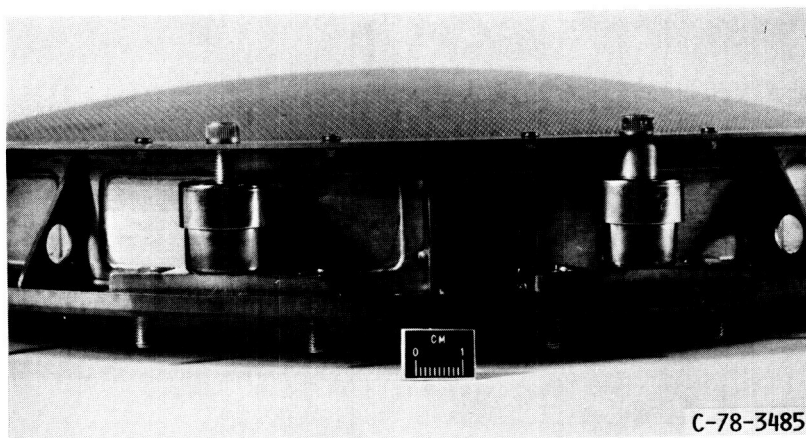


FIGURE 3. - 900-SERIES ELECTRODE ASSEMBLY.

ORIGINAL PAGE
BLACK AND WHITE PHOTOGRAPH

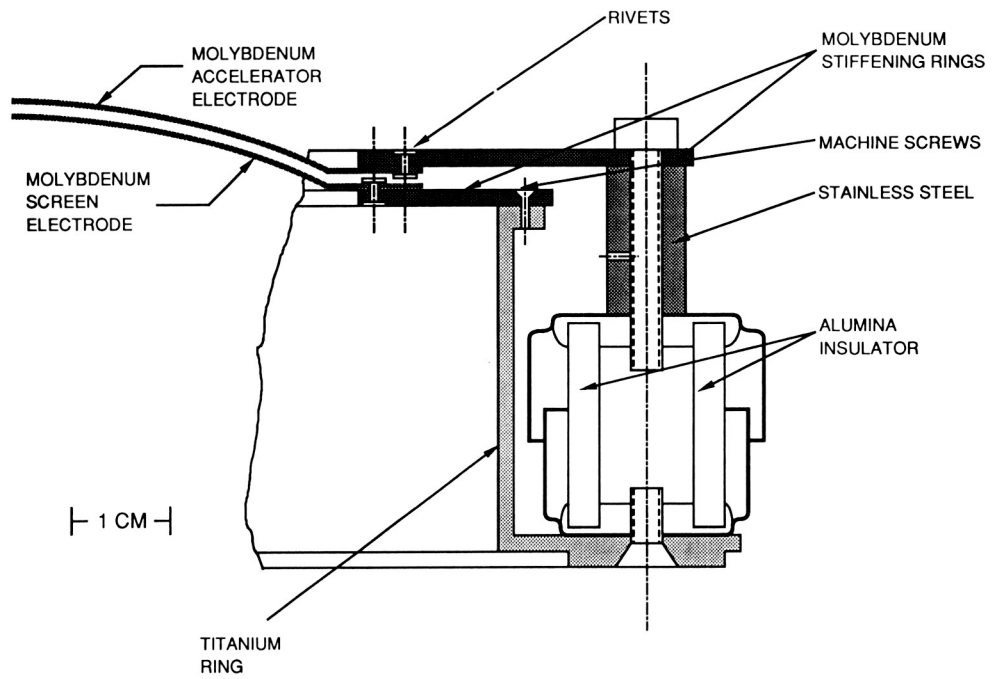


FIGURE 4. - J-SERIES ELECTRODE ASSEMBLY.

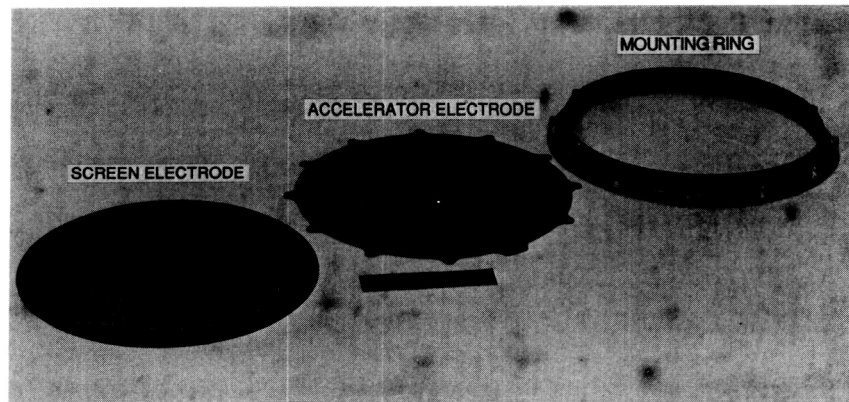


FIGURE 5. - J-SERIES ELECTRODE ASSEMBLY COMPONENTS.

ORIGINAL PAGE
BLACK AND WHITE PHOTOGRAPH

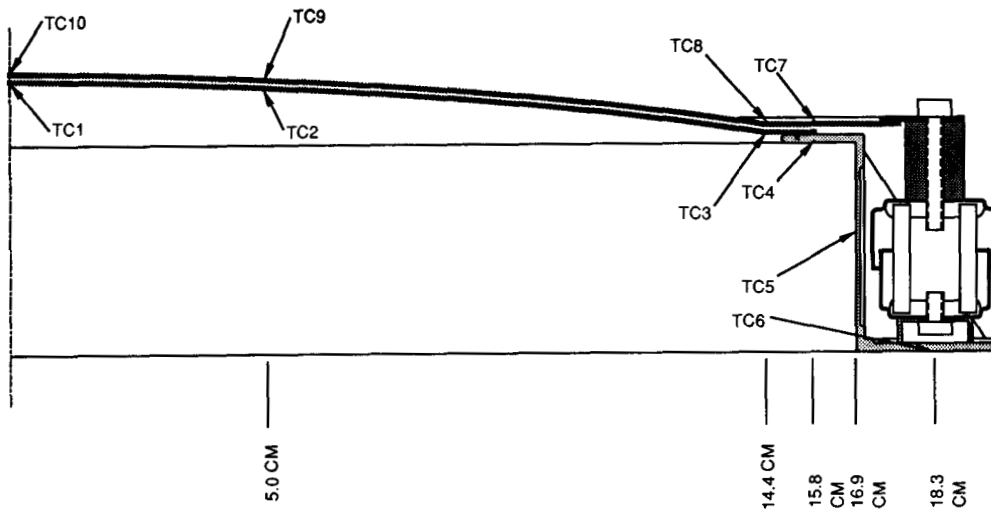


FIGURE 6. - THERMOCOUPLE LOCATIONS ON THE 900-SERIES SN813 ASSEMBLY.

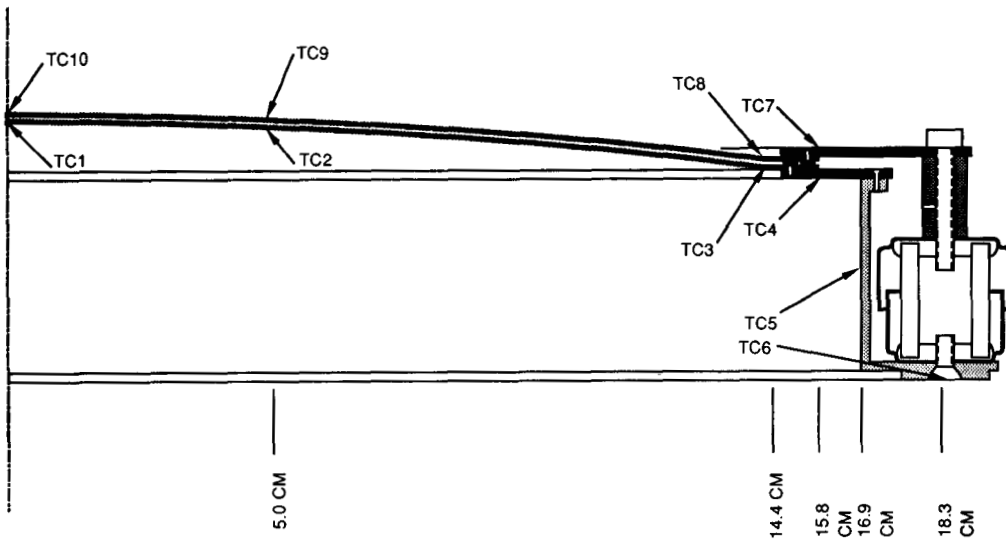


FIGURE 7. - THERMOCOUPLE LOCATIONS ON THE J-SERIES SN842 ASSEMBLY.

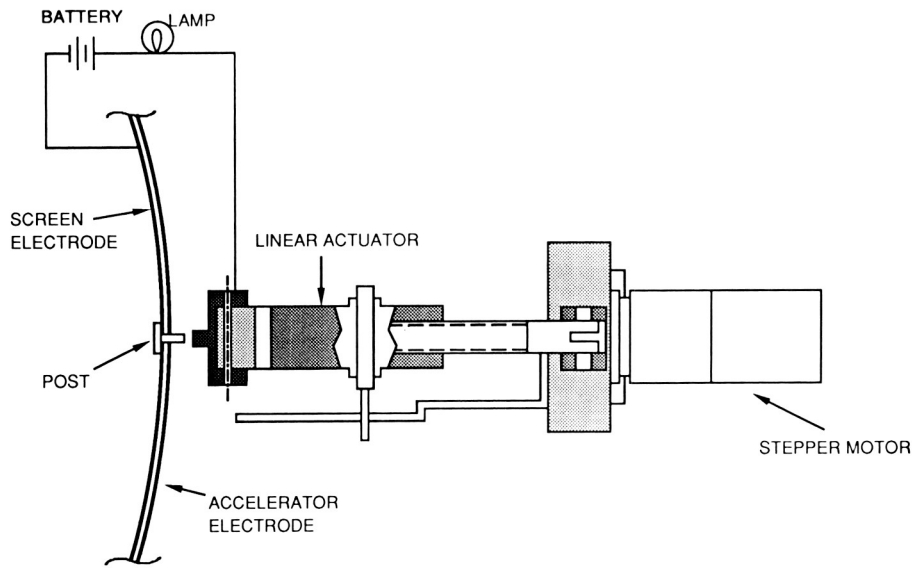


FIGURE 8. - SCREEN ELECTRODE MEASURING SYSTEM SCHEMATIC.

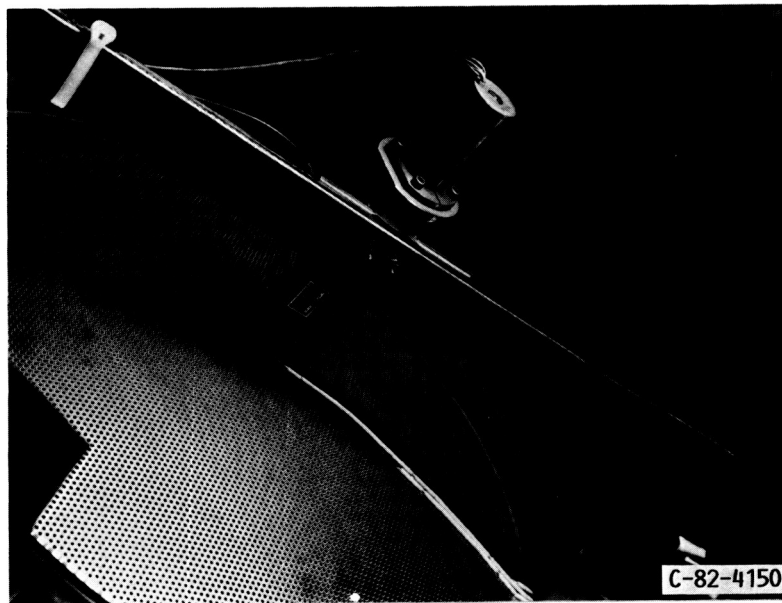


FIGURE 9. - DISPLACEMENT MEASUREMENT PROBE ASSEMBLY.

ORIGINAL PAGE
BLACK AND WHITE PHOTOGRAPH

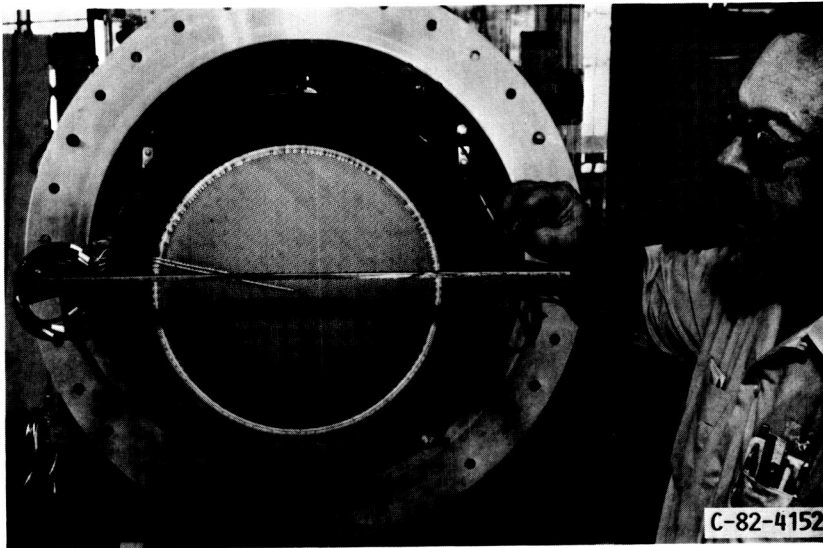


FIGURE 10. - DISPLACEMENT MEASUREMENT ASSEMBLY.

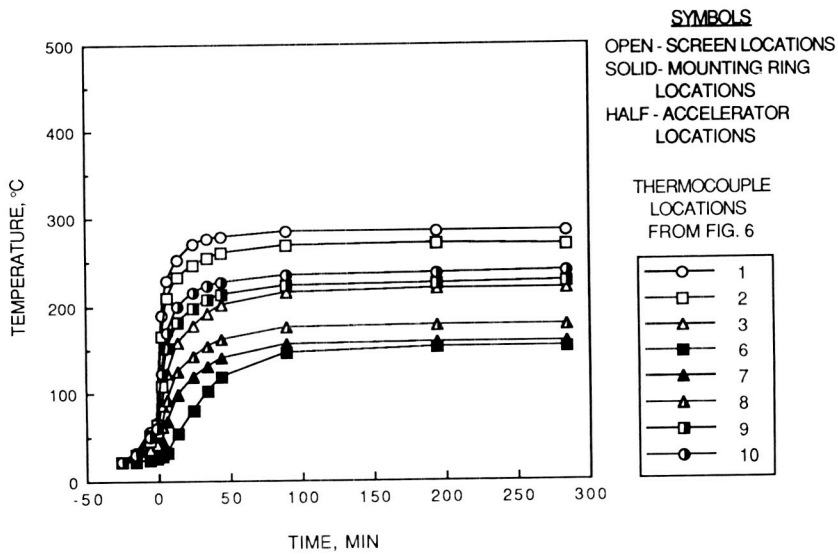


FIGURE 11. - 900-SERIES ASSEMBLY TRANSIENT TEMPERATURES AT 210 W DISCHARGE POWER.

ORIGINAL PAGE
 BLACK AND WHITE PHOTOGRAPH

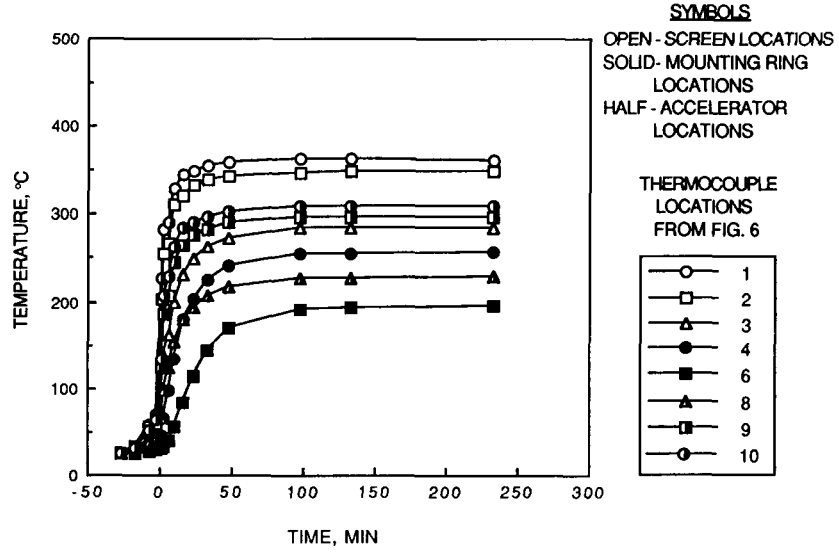


FIGURE 12. - 900-SERIES ASSEMBLY TRANSIENT TEMPERATURES AT 350 W DISCHARGE POWER.

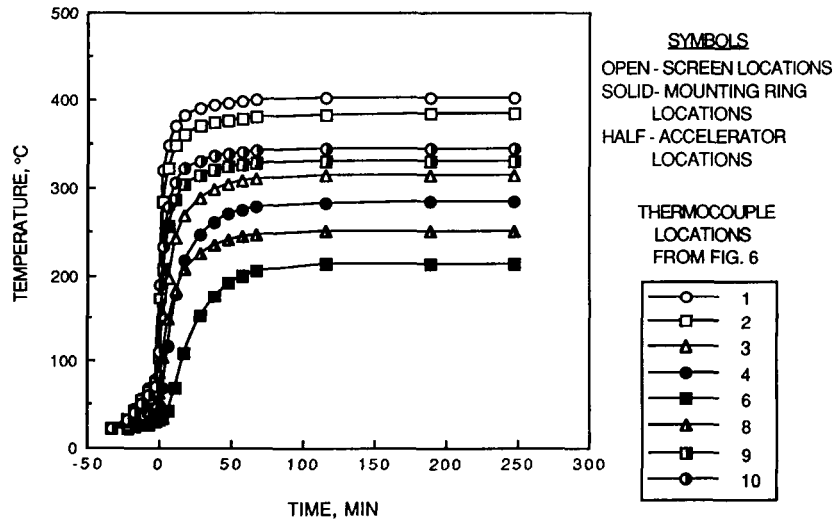


FIGURE 13. - 900-SERIES ASSEMBLY TRANSIENT TEMPERATURES AT 493 W DISCHARGE POWER.

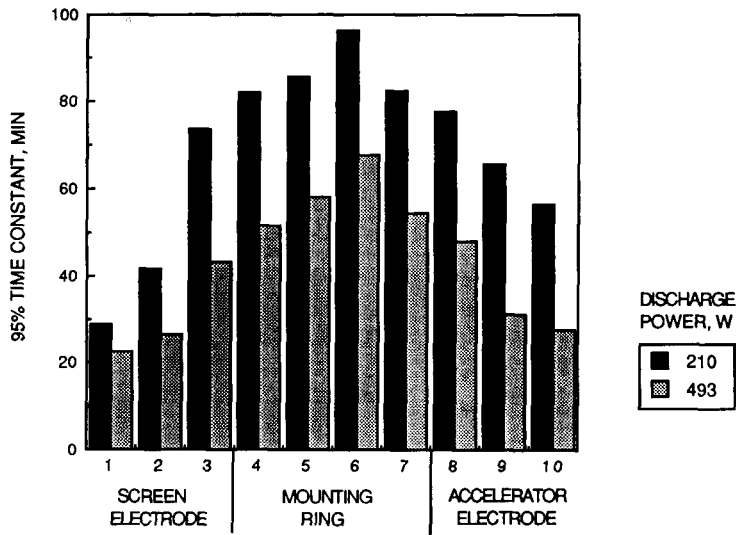


FIGURE 14. - 95% TIME CONSTANT FOR A 900-SERIES ASSEMBLY (THERMOCOUPLE LOCATION FROM FIGURE 6).

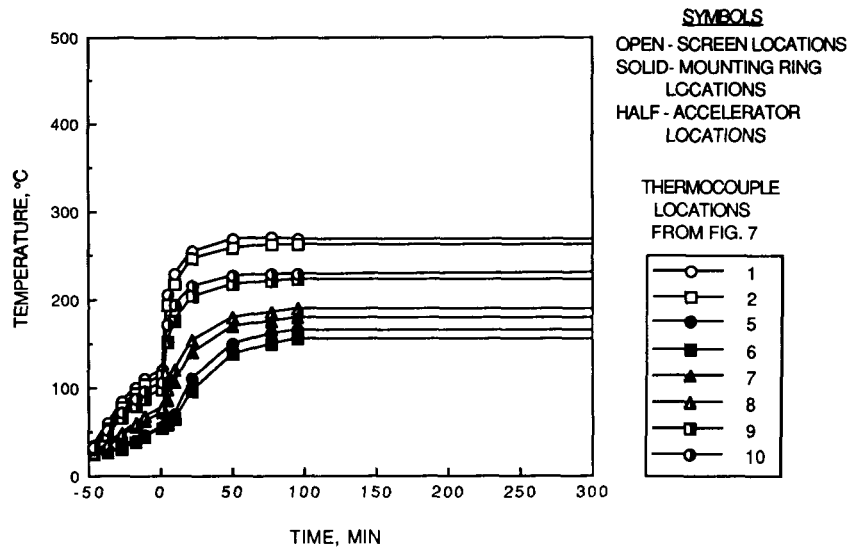


FIGURE 15. - TRANSIENT TEMPERATURES OF A J-SERIES ASSEMBLY AT 210 W.

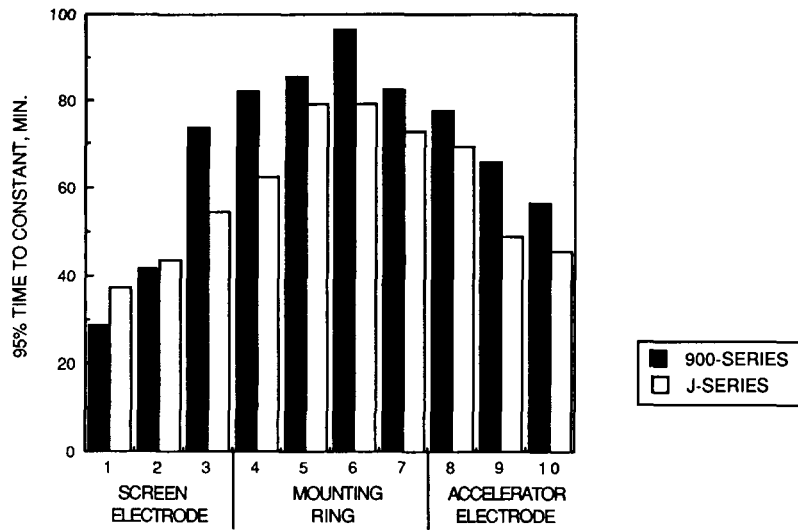


FIGURE 16. - COMPARISON OF 95% TIME CONSTANTS FOR A 900 AND J-SERIES ASSEMBLY AT 210 W (THERMOCOUPLE NUMBER FROM FIGS. 6 AND 7).

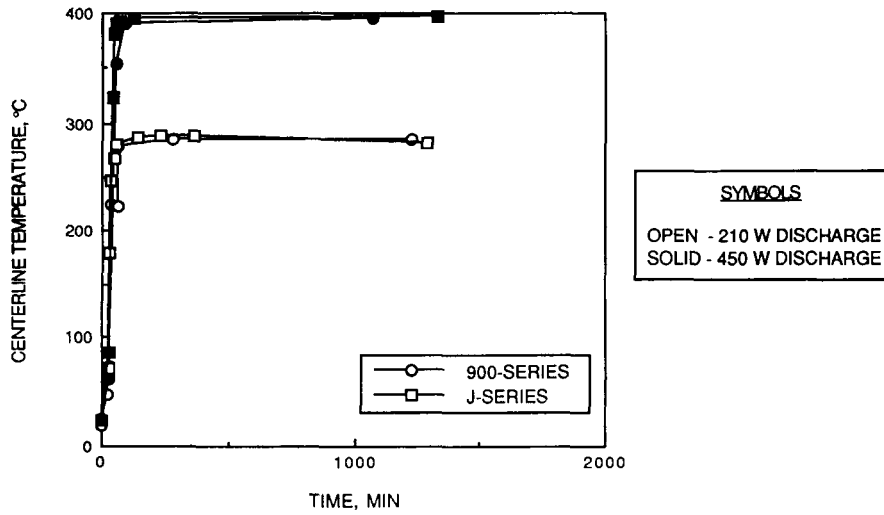


FIGURE 17. - COMPARISON OF TRANSIENT SCREEN ELECTRODE CENTERLINE TEMPERATURES FOR 900 AND J-SERIES.

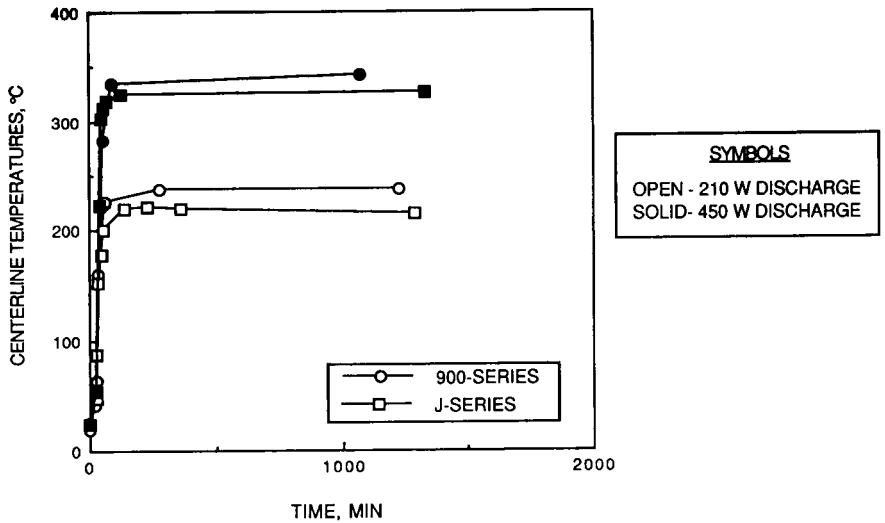


FIGURE 18. - COMPARISON OF TRANSIENT ACCELERATOR ELECTRODE CENTERLINE TEMPERATURES FOR 900 AND J-SERIES.

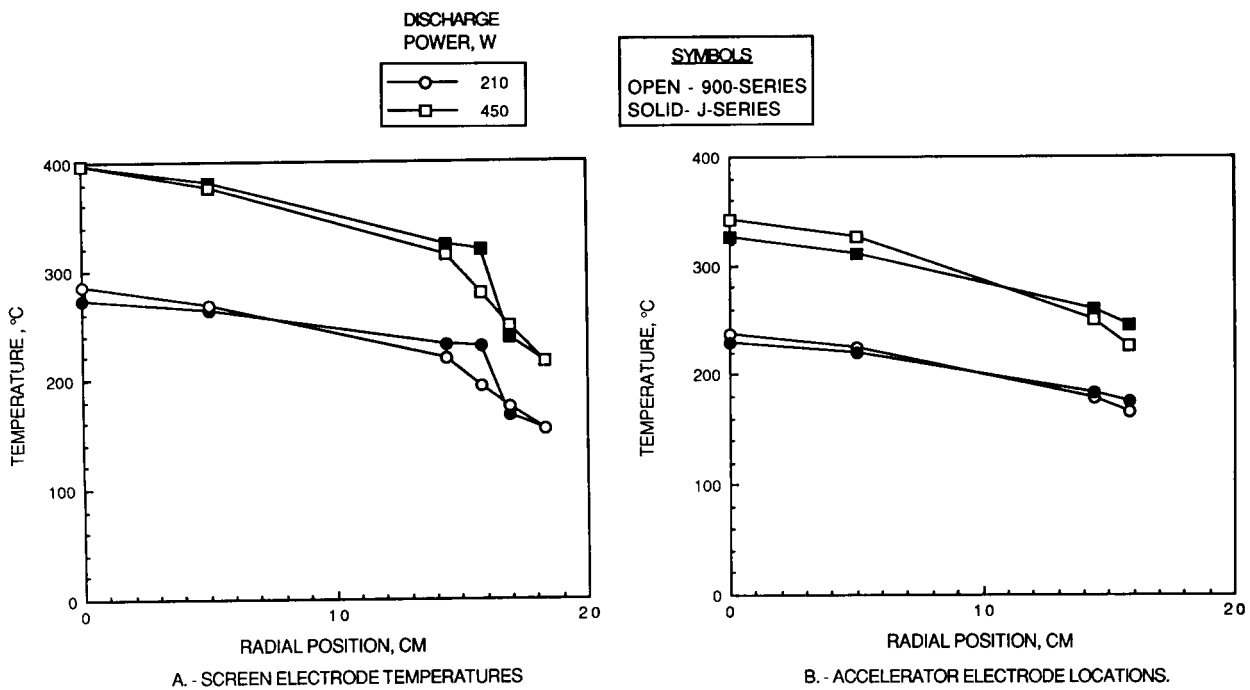
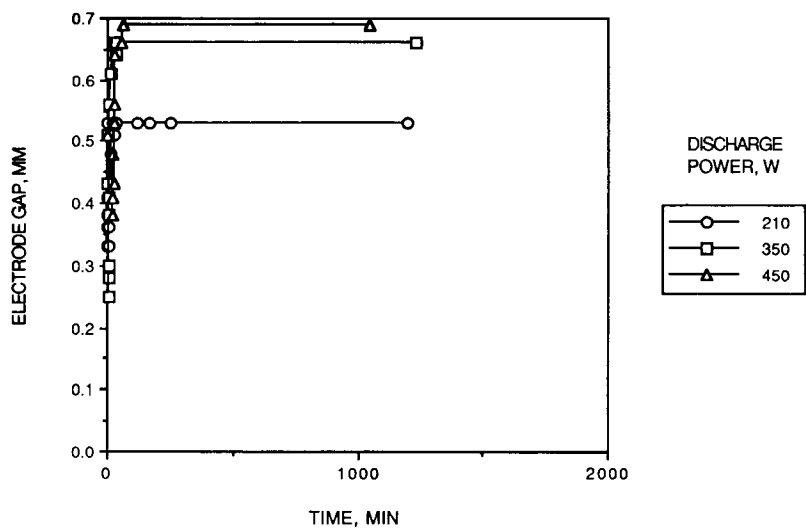
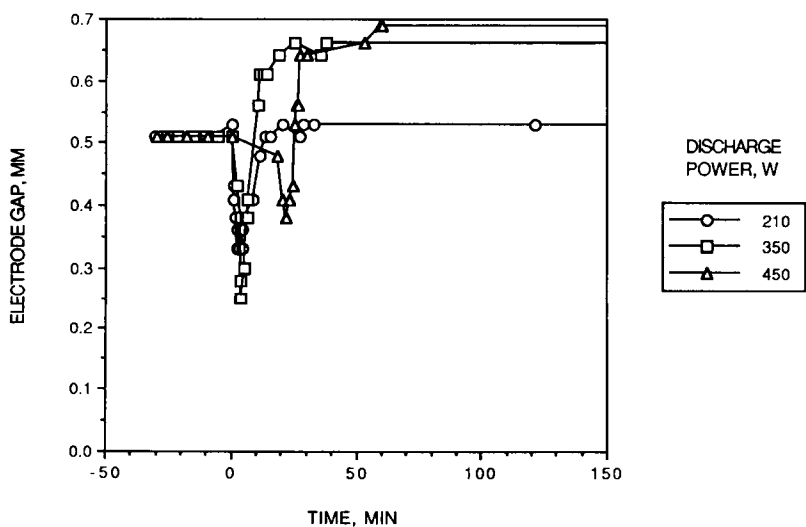


FIGURE 19. - EQUILIBRIUM TEMPERATURE PROFILES.

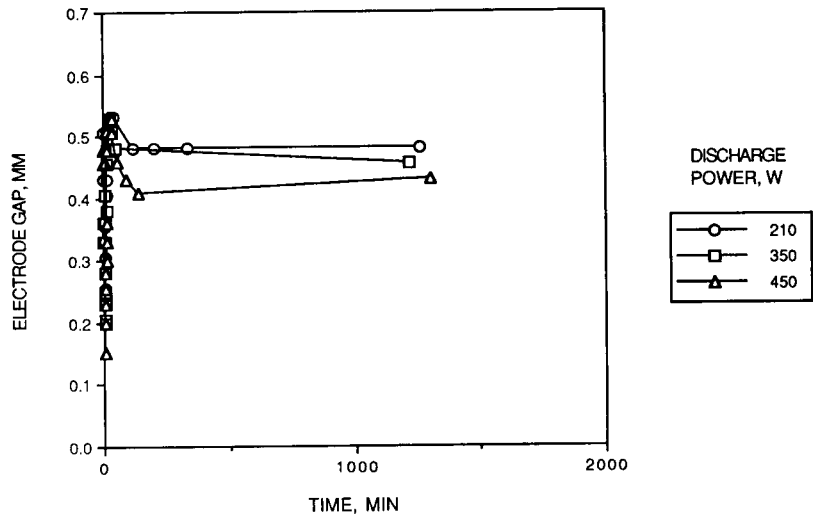


A. - LONG TERM EQUILIBRATION TRANSIENT

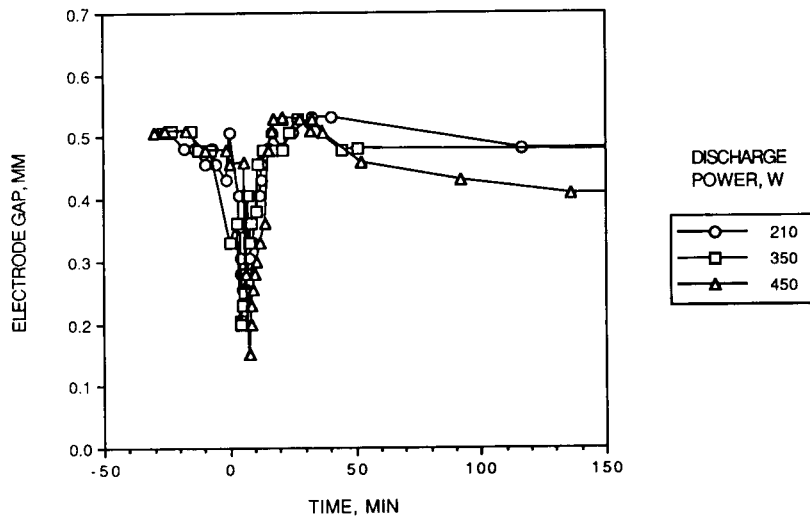


B. - SHORT TERM HEATING TRANSIENT

FIGURE 20. - 900-SERIES SN813 TRANSIENT ELECTRODE GAP.



A. - LONG TERM EQUILIBRATION TRANSIENT.



B. - SHORT TERM HEATING TRANSIENT.

FIGURE 21. - J-SERIES SN842 TRANSIENT ELECTRODE GAP.

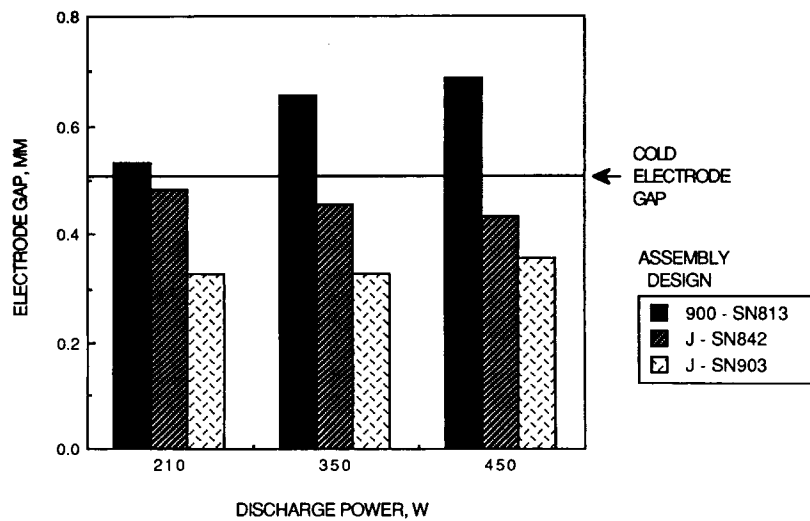


FIGURE 22. - EQUILIBRIUM ELECTRODE GAP FOR THREE ASSEMBLIES.



Report Documentation Page

1. Report No. NASA TM-102124 AIAA-89-2719		2. Government Accession No.		3. Recipient's Catalog No.	
4. Title and Subtitle Structural and Thermal Response of 30 cm Diameter Ion Thruster Optics				5. Report Date	
				6. Performing Organization Code	
7. Author(s) G.S. MacRae, R.J. Zavesky, and S.T. Gooder				8. Performing Organization Report No. E-4904	
				10. Work Unit No. 506-42-31	
9. Performing Organization Name and Address National Aeronautics and Space Administration Lewis Research Center Cleveland, Ohio 44135-3191				11. Contract or Grant No.	
				13. Type of Report and Period Covered Technical Memorandum	
12. Sponsoring Agency Name and Address National Aeronautics and Space Administration Washington, D.C. 20546-0001				14. Sponsoring Agency Code	
15. Supplementary Notes Prepared for the 25th Joint Propulsion Conference cosponsored by the AIAA, ASME, SAE, and ASEE, Monterey, California, July 10-12, 1989.					
16. Abstract This paper presents tabular and graphical data intended for use in calibrating and validating structural and thermal models of ion thruster optics. A 30 cm diameter, two electrode, mercury ion thruster was operated using two different electrode assembly designs. With no beam extraction, the transient and steady state temperature profiles and center electrode gaps were measured for three discharge powers. The data showed that the electrode mount design had little effect on the temperatures, but significantly impacted the motion of the electrode center. Equilibrium electrode gaps increased with one design and decreased with the other. Equilibrium displacements in excess of 0.5 mm and gap changes of 0.08 mm were measured at 450 W discharge power. Variations in equilibrium gaps were also found among assemblies of the same design. The presented data illustrate the necessity for high fidelity ion optics models and development of experimental techniques to allow their validation.					
17. Key Words (Suggested by Author(s)) Ion engine Ion optics Structural analysis Finite element analysis			18. Distribution Statement Unclassified - Unlimited Subject Category 20		
19. Security Classif. (of this report) Unclassified		20. Security Classif. (of this page) Unclassified		21. No of pages 28	22. Price* A03